Multimodal Segmentation of Brain tumor using BraTS dataset 2020

Author
Aniqa Saeed

Regn Number

00000318299

Supervisor

Dr. Amer Sohail Kashif

DEPARTMENT OF BIOMEDICAL ENGINEERING AND SCIENCES
SCHOOL OF MECHANICAL & MANUFACTURING ENGINEERING
NATIONAL UNIVERSITY OF SCIENCES AND TECHNOLOGY
ISLAMABAD, PAKISTAN

May 2023

Multimodal Segmentation of Brain tumor using BraTS dataset 2020

Author

Aniqa Saeed

Regn Number

00000318299

A thesis submitted in partial fulfillment of the requirements for the degree of

MS Biomedical Sciences

Thesis Supervisor:

Dr.Amer Sohail Kashif

Thesis Supervisor's Signature:

_____

DEPARTMENT OF BIOMEDICAL ENGINEERING AND SCIENCES

SCHOOL OF MECHANICAL & MANUFACTURING ENGINEERING

NATIONAL UNIVERSITY OF SCIENCES AND TECHNOLOGY

ISLAMABAD, PAKISTAN

May 2023

Copyright Statement

- Copyright in text of this thesis rests with the student author. Copies (by any process) either in full, or of extracts, may be made only in accordance with instructions given by the author and lodged in the Library of NUST School of Mechanical & Manufacturing Engineering (SMME). Details may be obtained by the Librarian. This page must form part of any such copies made. Further copies (by any process) may not be made without the permission (in writing) of the author.
- The ownership of any intellectual property rights which may be described in this thesis is vested in NUST School of Mechanical & Manufacturing Engineering, subject to any prior agreement to the contrary, and may not be made available for use by third parties without the written permission of the SMME, which will prescribe the terms and conditions of any such agreement.
- Further information on the conditions under which disclosures and exploitation may take place is available from the Library of NUST School of Mechanical & Manufacturing Engineering, Islamabad.

Dedication

Dedicatedtomybeloved Parents
‘Mr. &Mrs.Muhammad Saeed’

Acknowledgments

First and foremost, I am thankful to Allah Subhana Watala, the most gracious and most merciful for His blessings given to me and for guiding me throughout this work. I could have nothing without Your priceless help and guidance. Whoever helped me throughout the course of my thesis, whether my parents, siblings, and friends, it was your will, so indeed none be worthy of praise but you.

I am profusely thankful to my beloved parents who raised me when I was not capable of walking and continued to support me throughout in every step of my life.

I would like to express my profound gratitude and special thanks to my supervisor Dr. Amer Sohail kashif, for his unwavering support and advice during my thesis, as well as for providing me with resources for my research. I am thankful to him for assisting me in learning and for giving me his precious time and attention.

I am especially thankful to Dr. Syed Omer Gillani for his tremendous support and cooperation. Each time I got stuck in something, he came up with solution. Without his support I wouldn't have been able to complete my thesis. I appreciate his patience and guidance throughout the whole thesis.

I am thankful to Dr. Asim waris & Dr. Javaid Iqbal for their constant support and continuous guidance throughout the whole journey of this project. I really appreciate the compassion, kindness, and assistance of my all thesis GEC members throughout my research work. I am thankful to Dr. Rizwan Uppal who supported me throughout my research work and providing me sources for it.

I am thankful to all siblings, my beloved brother and sisters for their treasured support and unwavering faith in me. They have always been a great source of inspiration for me. Special thanks to my brother Farhan, whose one call was enough for me to keep me motivated in all this tough time.

Finally but very wholeheartedly thanks to Zohaib, for being there with me and motivating me to continue when where I decided to back-off. I would like to express my gratitude to all individuals who have rendered valuable assistance to my study.


بسم الله الرحمن الرحيم

Abstract

BRaTS'20 dataset aims for better understanding and developing an AI-based approach with novelty for multimodal segmentation of brain tumor using MRI images that are already in use since 2015 for better and accurate diagnosis of brain tumor. Pre-operative multimodal MRI scans of glioblastoma (GBM/HGG) and lower grade glioma (LGG), with pathologically confirmed diagnosis are available for each year where AI students are welcomed for challenges to develop novel models. These datasets contain training, validation and testing data for respective year's BraTS challenge. Our study involve automated segmentation using SegResNet model for 3T multimodal MRI scans of recently provided BraTS dataset 2020. Our model has been designed based on the encoder-decoder structure and is able to achieve a 0.90 mean dice score on training set and 0.87 on the validation set. Experimental results on the testing set demonstrate no over or under fitting and is able to achieve average dice scores of 0.9000, 0.8911 and 0.8426 for the tumor core, whole tumor and enhancing tumor respectively. The proposed BraTS model underwent through some specific modifications that created novelty comparing datasets and models of previous benchmarks.Our approach has surpassed the previous models of BraTS'20 dataset in many ways giving highest dice scores for tumor core and enhancing tumor while second highest for whole tumor.

Keywords: Brain Tumor Segmentation, Deep Learning, SegResNet, BraTS 2020

TABLE OF CONTENT

Table of Contents

List of Figures

List of Tables

Abbreviations

AI	Artificial Intelligence
BRATS	Multimodal Brain Tumor Image Segmentation Benchmark
CBICA	Center of Biomedical Image Computing and Analytics
CNN	Convolutional Neural Network
CT	Computed Tomography
DL	Deep Learning
DSC	Dice score coefficient
DNN	Deep Neural Network
ET	Enhancing Tumor
FLAIR	Fluid Attenuation Inversion Recovery
GN	Group Normalization
HGG	High Grade Glioma
LGG	Low Grade Glioma
MICCAI	Medical Image Computing and Computer Assisted Intervention Society
ML	Machine Learning
MRI	Magnetic Resonance Imaging
RELU	Rectified Linear Unit
SEGRESNET	Semantic Segmentation Model
SVM	Support Vector Machines
T1	Longitudinal Relaxation Time
T2	Transverse Relaxation Time
T1-CE	Longitudinal Relaxation Time contrast enhanced
TC	Tumor Core
WHO	World Health Organization
WT	Whole Tumor

CHAPTER1

INTRODUCTION

INTRODUCTION

1.1 Gliomas

Gliomas are known as the primary cause of brain death and are most common types of primary brain tumors. They develop in the glial cells and can be of two main types. LGG, low grade gliomas (slow growing) and HGG, high grade gliomas (fast growing) **(Al-Dhahir 2022)**Treatment depends upon the condition and type of gliomas and its early detection. Automatic three dimensional brain tumor segmentation can save doctors time and can provide an appropriate method of additional tumor analysis. In USA, about 19,000 cases of new gliomas are diagnosed per year. Considering high US population rate, this statistic ratio is about a glioma incidence rate of 0.00064whichmeans 0.0064% or 6.4 cases per 100,000 populations have been appeared so far. Some data explains increased rate of gliomas in recent years in US, probably because researchers are now working more on it for accurate diagnosis. **(Tamimi AF 2017 Sep 27)**

In past years, about 16 reported cases **(Kelly 2010)**have been found after a clear focus on CNS which was detected by CT scan and MRI images. Concerning point was that individuals in these cases were asymptomatic. A more conservative study of 1000in the Journal of the American Medical Association (JAMA) detected three glioma cases out of 1000asymptomatic volunteers.**(Kelly 2010, Michael Goetz and Barbara Bobek-Billewicz 2016)**

1.2 Brain and Gliomas

The brain is the most complex organ in the human body and is responsible for controlling all of the body's functions. It is divided into several different regions, each with its own unique functions and structures. The cerebrum is the largest part of the brain and is responsible for controlling conscious thought, movement, and sensation. It is divided into two hemispheres, the left and right, which are connected by a thick band of nerve fibers called the corpus callosum. The cerebellum, located at the base of the brain, is responsible for controlling movement and coordination. It also plays a role in maintaining balance and posture. The brainstem is located at the base of the brain and connects the brain to the spinal cord. It controls many of the body's basic functions, including breathing, heart rate, and blood pressure.

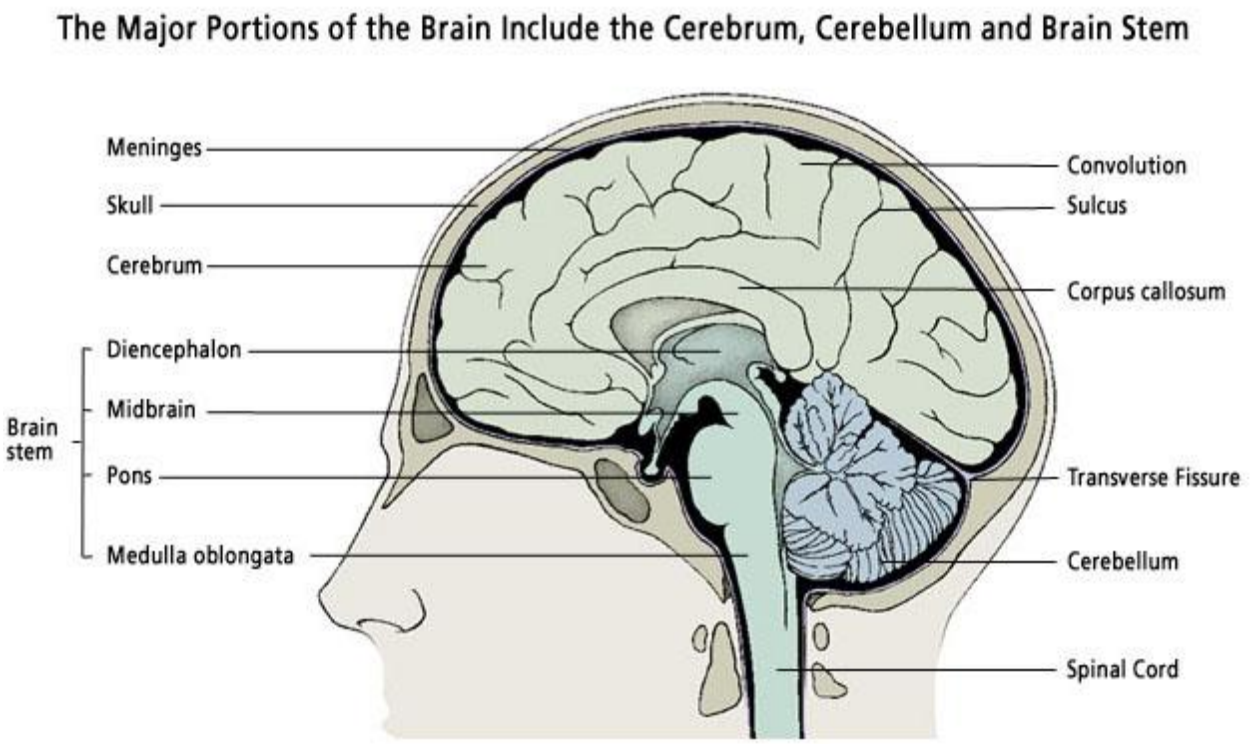

Figure 1: Brain Anatomy

The thalamus and hypothalamus are located in the center of the brain and play important roles in regulating the body's internal environment, including temperature, hunger, and thirst. The limbic system, located deep within the brain, plays a key role in controlling emotions, motivation, and memory. Overall, the brain is a complex and intricate organ that plays a critical role in controlling all aspects of the body's functions.

1.2.1 Major site of Glioma

Gliomas can develop in various regions of the brain, and the location of the tumor can impact the symptoms and treatment options.

Some of the major sites of gliomas include:

- ***Cerebrum****:* The most common location for gliomas is in the cerebrum, which is the largest part of the brain responsible for conscious thought, movement, and sensation. Gliomas in this region can cause symptoms such as seizures, headaches, and changes in mental status.

- ***Brainstem:*** Gliomas in the brainstem can cause symptoms such as difficulty with coordination, weakness, and problems with breathing or heart rate.
- ***Cerebellum***: Gliomas in the cerebellum can cause symptoms such as problems with balance and coordination, as well as headaches and nausea.
- ***Spinal cord:*** Gliomas can also develop in the spinal cord, which can cause symptoms such as weakness, numbness, and difficulty with coordination.

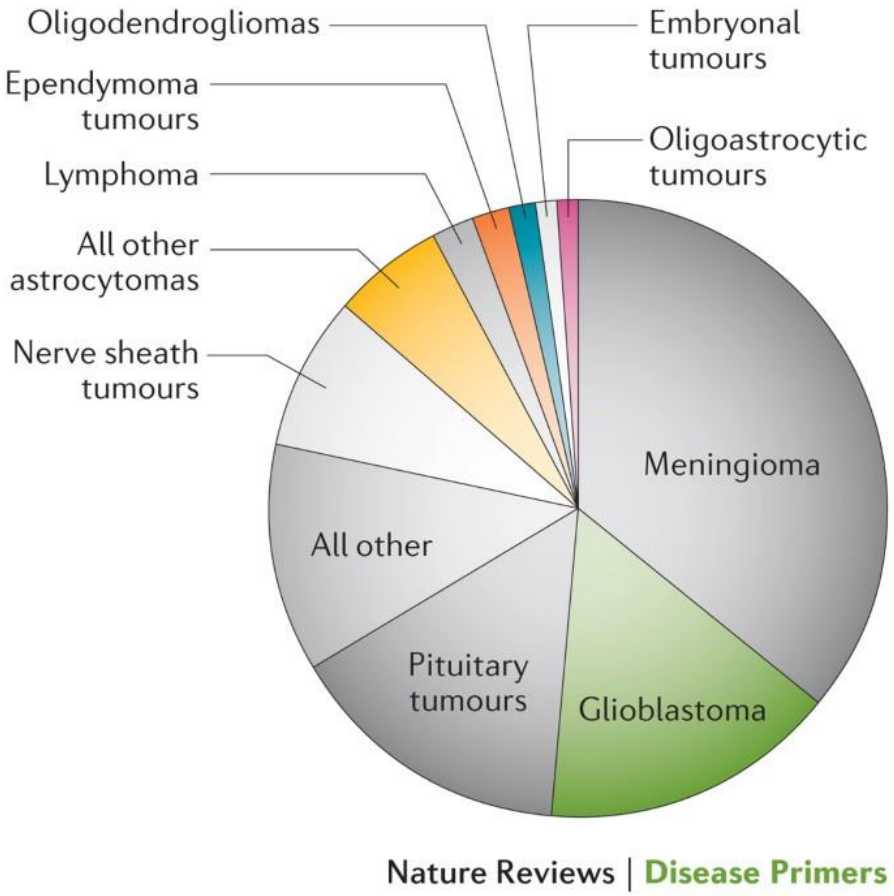

Figure 2: Statistical review of sites of Glioma

1.3 Pathology of Gliomas

Gliomas are a type of brain tumor that develops from the glial cells, which provide support and insulation for the neurons in the brain. The pathology of gliomas involves the abnormal growth and division of glial cells, which can lead to the formation of a tumor. These tumors can compress and damage surrounding brain tissue, leading to a range of symptoms such as

headaches, seizures, and changes in mental status.The pathology of gliomas is complex and can involve genetic mutations and alterations in signaling pathways that contribute to abnormal cell growth and division.

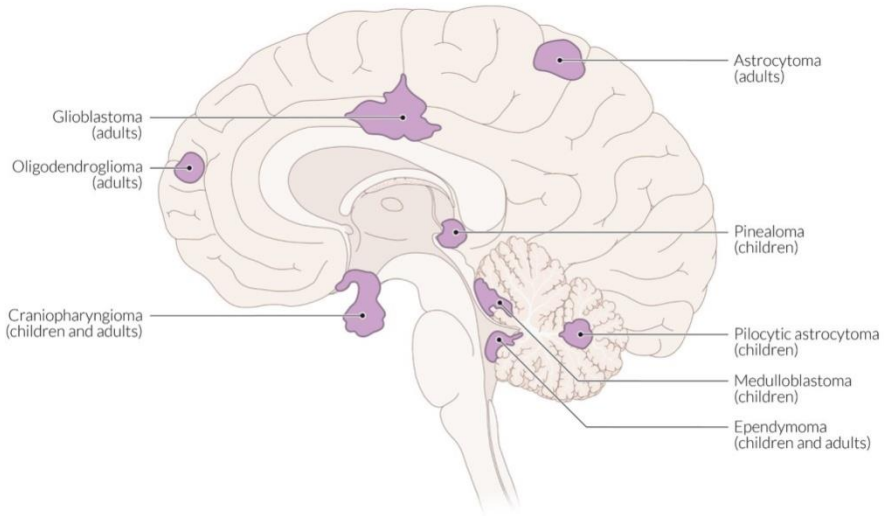

Figure 3: Pathological Site of Gliomas

1.4 Classification of Gliomas

Gliomas are classified based on their characteristics, including their location in the brain, histological features, genetic mutations, and clinical behavior. The World Health Organization (WHO) has developed a classification system for gliomas based on these factors, which ranges from grade I to grade IV:

- ***Grade I:*** These are the least aggressive and slow-growing tumors, and they often have a good prognosis. They are also known as pilocyticastrocytomas, and they typically occur in children and young adults.
- ***Grade II:*** These are low-grade tumors that tend to grow slowly, but they can become more aggressive over time. They are also known as diffuse astrocytomas or oligodendrogliomas, and they often occur in adults.
- ***Grade III:*** These are intermediate-grade tumors that tend to grow more quickly than grade II tumors. They are also known as anaplastic astrocytomas or oligodendrogliomas,

and they can occur in both children and adults.

- ***Grade IV:*** These are the most aggressive and fast-growing tumors, and they have a poor prognosis. They are also known as glioblastomas, and they can occur in both children and adults.

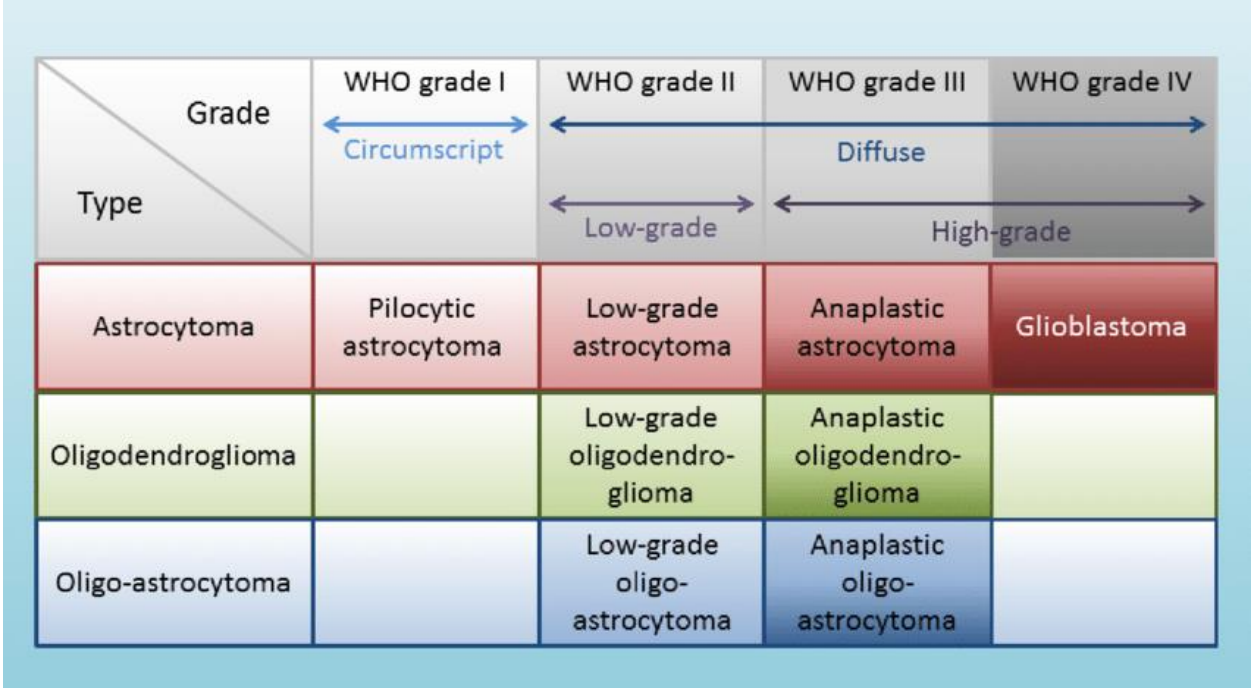

Table 1: WHO Grading & Classification of Gliomas

1.5 Signs and Symptoms

Common signs and symptoms of gliomas include

- Headache
- Nausea or vomiting
- Confusion or a decline in brain function
- Memory loss
- Personality changes or irritability
- Difficulty with balance
- Urinary incontinence
- Vision problems, such as blurred vision, double vision or loss of peripheral vision
- Speech difficulties **(F. P. Polly 2018)**

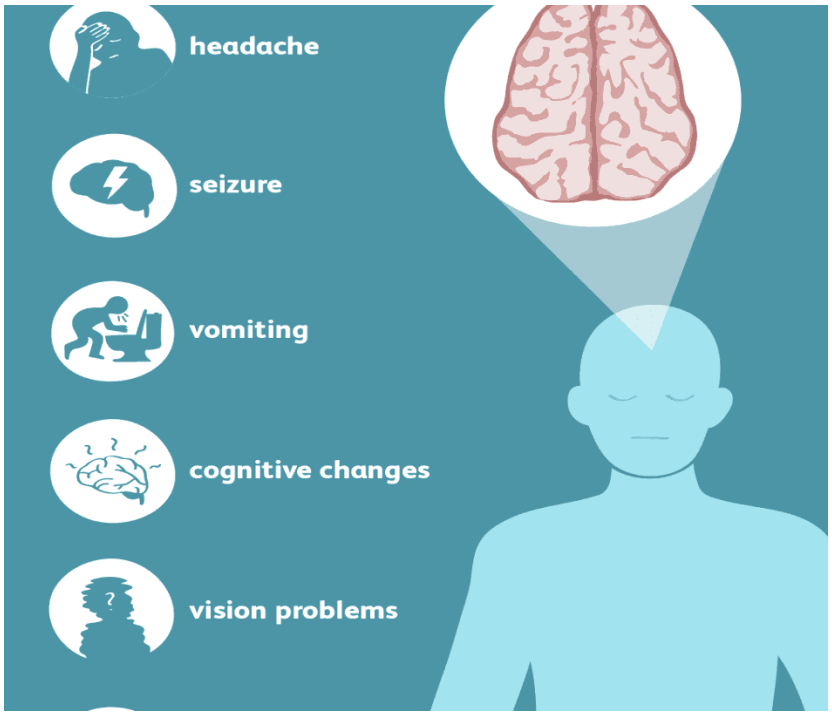

Figure 4: Signs and Symptoms of brain gliomas

1.6 Diagnostic Methods

Some important diagnostic methods that have been used worldwide include Biopsy, Tumor markers, PET scan, CT scan specially CT cerebral angiogram and magnetic resonance imaging MRI.**(Yue Cao 2006, Kelly 2010, Tamimi AF 2017 Sep 27, Al-Dhahir 2022)**

Magnetic resonance imaging provides unremarkable soft tissue differentiation and in vivo assessment of pathological, physiologic and metabolic properties of enhancing tissue.**(Yue Cao 2006)** Many diagnostic and imaging modalities for glioma diagnosis are known but for the accurate and timely diagnosis after defining tumor volumes, planning radiation and other treatment keeping in mind the re-optimization of treatment plan, it is a major task to select the imaging modality that will reduce glioma spreading and will lead to a better prognosis after detection.**(Yuille 2018, Philipp Kickingereder 2019)**Major sequences used for glioma detection include T1, T2, T1ce and Flair images.

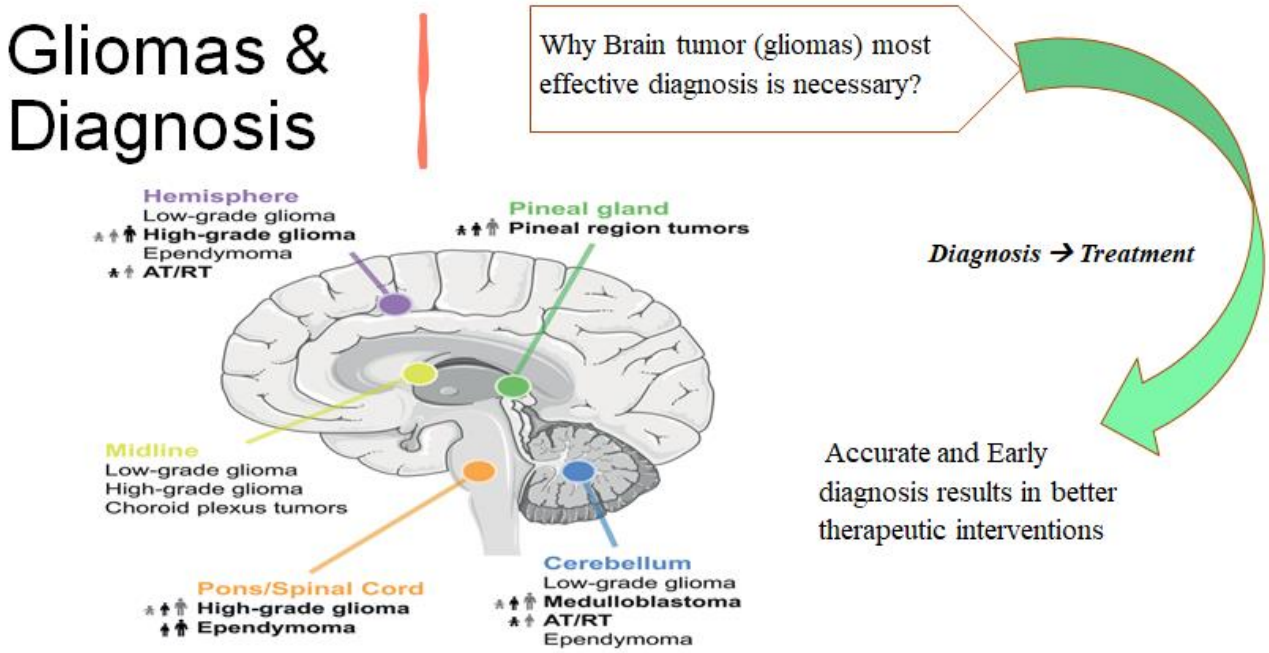

Figure 5: Glioma sites & Diagnosis

1.7 Magnetic Resonance Imaging (MRI)

MRI is considered to be a very important and non-invasive imaging modality for early glioma detection. **(F. P. Polly 2018)** and grading of supra-tentorial gliomas with high sensitivity and specificity. It is considered a non-invasive method and is useful in cases where the biopsy procedure is a contraindication or rejected by the patient.Conventional magnetic resonance imaging with T1, T2, FLAIR, and contrast enhancement are basic tests for its diagnosis and determine its grade.

Among the major parameters of tumor and necrotic tissue, peri-tumoral edema, a hyper-intense T2-weighted signal around Enhancing Tumor on MRI images, perforates into the parenchymal extracellular space. **(Yue Cao 2006, Jin Liu 2014)**This makes the differentiation of necrotic tissue and vasogenic edema difficult.**(Bjoern H. Menze 2014, Spyridon Bakas 2017, Spyridon Bakas 2019)**Considering these limitations and important parameters in glioma detection, Therefore, BraTS datasets using 3T multimodal MRI brain images for glioma detection are widely used by researchers every year for better diagnosis reducing the rates of late detections.

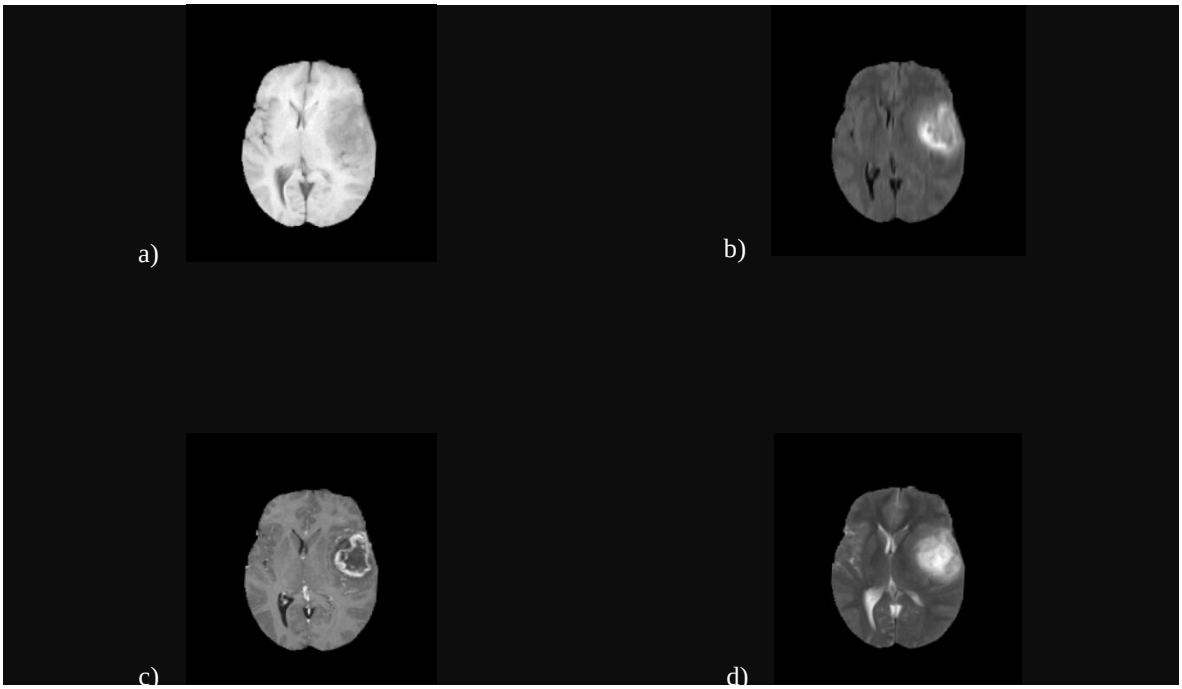

Figure 6: Four imaging modalities: (a) T1-weighted MRI (b) T2-weighted MRI (c) T1-weightedontrast enhanced MRI and (d) FLAIR with contrast enhancement (Jin Liu 2014)

1.8 Role of Deep Learning (DL) in Brain Tumor segmentation

Deep learning is an important technique for the analysis of brain tumor majorly glioms, by using MRI images. Recently, Deep learning approaches have consistently outperformed traditional brain tumor segmentation methods. **(Dinthisrang Daimary 2019)** Medical image segmentation for detection of brain tumor from the MRI images is a very important process for deciding right therapy at the right time because the earlier the detection, the faster the treatment can be started. **(Crimi 2015)**

Peri-tumoral edema, characterized by a hyper-intense T2-weighted signal surrounding the enhancing tumor on MRI images, is a significant parameter for evaluating tumor and necrotic tissue. This edema can extend into the extracellular space of the parenchyma. [8, 11] This makes the differentiation of necrotic tissue and vasogenic edema difficult.[12-14] Considering these limitations and important parameters in glioma detection, MRI is considered to be a very important and non-invasive imaging modality for early glioma detection. [7] Therefore, BraTS datasets using 3T multimodal MRI brain images for glioma detection are widely used by

researchers every year for better diagnosis reducing the rates of late detections.

Deep learning is an important technique for the analysis of brain tumor majorly glioms, by using MRI images.

Some important models include Convolution Neural Networks (CNNs) **(Richard McKinley Oct 2019)**, Recurrent Neural Networks (RNNs) and Artificial Neural Networks (ANN). **(Amin Zadeh Shirazi 2020, Khushboo Munir 2022)** The first CNN based architecture that won the competition of ImageNet in 2012, known as AlexNet, **(Md Zahangir Alom 2018)**all preceeding network architectures started uses more number of layers to reduce error ratios. The drawback of this appeared when layers were increased due to some large dataset accomplishment, exploding gradient either became 0 or too large leading to increase in test set error rates.**(Changxing Ding 2019, Yue Zhang 2021)**

In order to solve this issue, ***SegResNet architecture*** was proposed in 2015 **(Olaf Ronneberger 2015, MAHNOOR ALI 2020, Muhammad Shafiq 2022)**with the concept of having Residual Blocks and skip connections. It helps in connecting different and large number of layers more efficiently by skipping some unnecessary layers forming a Residual block. **(Anuja Arora 2021)**These blocks are stacked altogether to make ResNet architecture that is used by most researchers now-a-days. **(Dinthisrang Daimary 2019, Amin Zadeh Shirazi 2020, Muhammad Shafiq 2022)**

1.9 Multi-modal brain tumor segmentation BraTS

The Brain Tumor Radiogenomics (BRATS) dataset is a collection of MRI scans of patients with brain tumors, along with clinical and genetic data. The dataset was created to support research in the field of radiogenomics, which involves the study of the relationship between imaging features of tumors and their underlying molecular characteristics.

The BRATS dataset includes MRI scans from over 200 patients with gliomas, which have been annotated by experts to identify regions of the brain that are affected by the tumor. The dataset also includes genetic and clinical data for some of the patients, which can be used to study the relationship between imaging features and underlying genetic mutations.

The BRATS dataset has been used in a variety of research studies, including the development of machine learning algorithms to predict the location and grade of gliomas based on MRI scans, as

well as the identification of imaging features that are associated with specific genetic mutations. The BRATS dataset is freely available for research purposes, and it can be accessed through the Medical Image Computing and Computer Assisted Intervention (MICCAI) Society. Researchers can use the dataset to develop and test new algorithms and techniques for analyzing brain tumor imaging data, with the goal of improving the accuracy of diagnosis and treatment for patients with brain tumors.

1.9.1 BraTS Dataset 2020 and Segmentation

The BRATS dataset is updated annually, with the most recent version being the BRATS 2020 dataset. The BRATS 2020 dataset is a collection of MRI scans of patients with brain tumors, along with clinical and genetic data, and it includes data from over 800 patients with gliomas.
In addition to the imaging data, the BRATS 2020 dataset includes genetic and clinical data for some of the patients, which can be used to study the relationship between imaging features and underlying genetic mutations. The dataset also includes benchmarks and evaluation metrics for researchers to assess the accuracy of their algorithms and techniques.
This study uses SegResNet architecture on publicly available dataset, which is preprocessed **(Rahimzadeh et al., 2021).** The data augmentation technique is applied to attain diversity. The image segmentation performance of BraTS 2020 using CNN-based methods can be improved by adopting data augmentation. The data set has been loaded in batches and pre-trained weights have been used. The transfer learning technique along with encoder-decoder architecture has been applied, for achieving the best accuracy and dice scores **(Shin et al., 2016).** After concatenating the last connection layer, the output comes as 0 for a normal image and 1 for a glioma infected image. Best checkpoints for each model are saved after training, which are then used for the evaluation of the proposed model. The accuracy and dice score have been calculated. Furthermore, feature visualization algorithm investigated glioma infected and normal images by generating heat maps.

1.10 Research Aim and Objective

The basic aim of the study is to propose a fully automated model for an accurate and rapid detection of low grade and high grade gliomas from MRI using deep learning. The implementation of deep learning frameworks in medical image segmentation is an important task. The basic objectives of the study are as under:

- Propose a light weight more accurate model that out-performs previously proposed models
- Achieve high DSC for training, test and validation sets along with all cores defined in later chapters
- Reduce the burden on radiologist by automatic, accurate detection and segmentation of disease
- Objective diagnostic

CHAPTER2

LITERATURE REVIEW

RELATEDWORK

2.1 Low grade and High grade gliomas (LGG & HGG)

LGG and HGG refer to low-grade gliomas and high-grade gliomas, respectively. Gliomas are a type of brain tumor that originates from glial cells, which are the cells that support and protect neurons in the brain.The history of LGG and HGG is intertwined with the history of brain tumor classification. In the early 20th century, brain tumors were classified based on their histological appearance, which meant that tumors were grouped based on their cell type and the features of the cells under the microscope.

In 1926, Bailey and Cushing proposed a new classification system for brain tumors that took into account the tumor's location, growth pattern, and the age and sex of the patient. They classified gliomas into three groups: fibrillary, protoplasmic, and gemistocytic astrocytomas.

LGGs are considered grade II tumors and are characterized by a slow growth rate and a relatively favorable prognosis. In contrast, HGGs are considered grade III or IV tumors and are characterized by a fast growth rate and a poor prognosis. The classification of LGG and HGG has evolved over time as our understanding of brain tumors has improved. Today, gliomas are classified based on their molecular profile, which can provide additional information about the tumor's behavior and help guide treatment decisions.

2.2 Mechanism of Invasion of Gliomas in Brain

The invasion of glioma is a complex process involving multiple cellular and molecular mechanisms. Here are some of the mechanisms involved in the invasion of glioma:

Cell adhesion molecules: Glioma cells use cell adhesion molecules such as integrins to interact with extracellular matrix (ECM) proteins and other cells. These interactions enable the glioma cells to migrate through the ECM and invade surrounding tissue.

- **Proteases:** Glioma cells secrete proteases such as matrix metalloproteinases (MMPs) and cathepsins, which can degrade ECM proteins and facilitate invasion. MMPs in particular are known to play a role in glioma invasion by cleaving ECM proteins and releasing growth factors that promote glioma cell migration.

- **Cytoskeleton rearrangement:** Glioma cells undergo changes in their cytoskeleton, which enables them to move through the ECM. Actin filaments and microtubules are rearranged to form structures such as lamellipodia and filopodia, which extend and contract to allow the cells to move.
- **Chemotaxis:** Glioma cells respond to chemical signals in their environment, such as gradients of growth factors and cytokines, by migrating towards regions of higher concentration. This process, known as chemotaxis, can direct glioma cells towards blood vessels, where they can invade the brain parenchyma.
- **Tumor microenvironment:** The tumor microenvironment plays a crucial role in glioma invasion, as it provides a supportive environment for the glioma cells to grow and invade. Immune cells and stromal cells in the microenvironment can secrete factors that promote glioma invasion and angiogenesis.

The process is complex and multifaceted, and further research is needed to fully understand the mechanisms involved and develop effective therapies to prevent or slow down glioma invasion.

2.2.1 Structure of Glioma

The structure of gliomas can vary depending on the type, grade, and location of the tumor. In general, gliomas are classified as either low-grade or high-grade based on their cellularity, mitotic activity, and degree of necrosis. Within each grade of glioma, there can be considerable variation in the structure and behavior of the tumor, as each tumor is unique and can have a different genetic makeup and response to treatment. Therefore, a thorough understanding of the structure and molecular characteristics of gliomas is important for accurate diagnosis and treatment planning.

Low-grade gliomas typically have a well-defined border and are composed of relatively uniform cells with minimal invasion into surrounding brain tissue. They are usually slow-growing and can be present for several years before causing significant symptoms. The most common types of low-grade gliomas are diffuse astrocytomas and oligodendrogliomas.

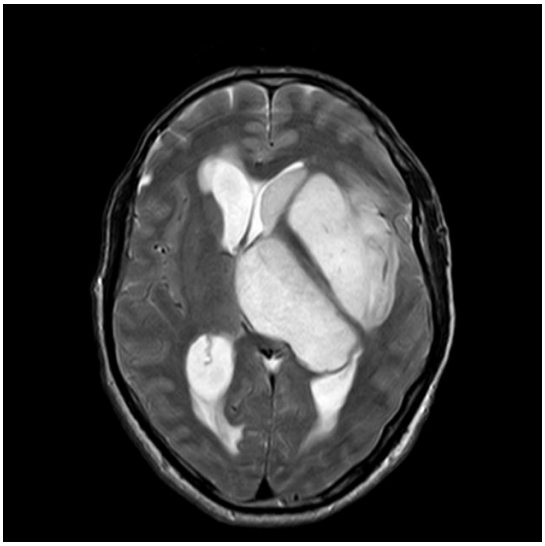

Figure 7: MRI image of a patient suffering from left sided LGG

High-grade gliomas, on the other hand, are more aggressive and invasive, with poorly-defined borders and a higher degree of cellular atypia and mitotic activity. They can rapidly infiltrate surrounding brain tissue, making complete surgical resection difficult, and have a higher likelihood of recurrence. The most common types of high-grade gliomas are glioblastomas and anaplastic astrocytomas.

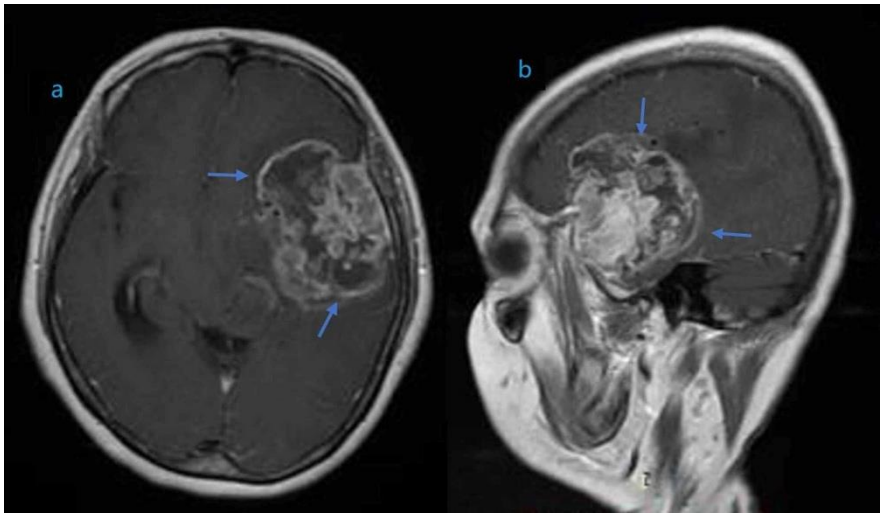

Figure 8: MRI axial & coronal image of a patient suffering from left sided HGG

2.3 Medical Image Segmentation

Medical image segmentation is the process of partitioning an image into multiple regions or segments based on the characteristics of the pixels within the image. In the context of medical imaging, image segmentation is used to identify and isolate specific anatomical structures or regions of interest within the image.

Medical image segmentation is a critical step in many clinical applications, including disease diagnosis, treatment planning, and image-guided interventions. For example, in neuroimaging, image segmentation can be used to identify and quantify the volume of specific brain structures, such as the hippocampus or the ventricles. In oncology, image segmentation can be used to delineate the boundaries of a tumor, which is essential for accurate treatment planning and monitoring.

2.4 Deep Learning and Image Segmentation

Deep learning is a subfield of artificial intelligence (AI), and the concept of using neural networks for learning from data dates back to the 1940s. However, the use of deep learning for medical image segmentation, including brain tumor segmentation, is a relatively recent development. The discovery of deep learning in the context of medical image segmentation can be attributed to the work of several researchers and research groups. One notable example is the U-Net architecture, which was proposed in 2015 by researchers at the University of Freiburg in Germany. U-Net is a deep learning architecture specifically designed for medical image segmentation, and it has been widely used for brain tumor segmentation.

2.4.1 DL and Brain tumor segmentation

Deep learning-based image segmentation has been used extensively for brain tumor segmentation in medical imaging. Here are some examples of its applications:

- ***Accurate tumor boundary delineation***: Deep learning-based image segmentation has enabled accurate and automated segmentation of brain tumors from medical images, improving the accuracy and reproducibility of tumor boundary delineation.
- ***Personalized treatment planning:*** Accurate tumor segmentation using deep learning can help clinicians plan more personalized treatment strategies for brain tumor

patients, by enabling them to accurately assess the size, location, and shape of the tumor.

- ***Assessment of treatment response:*** Deep learning-based image segmentation can be used to monitor the progression of brain tumors over time, enabling clinicians to assess treatment response and adjust treatment plans accordingly.
- ***Radiomics and machine learning:*** The use of deep learning-based image segmentation in conjunction with radiomics and machine learning techniques has enabled the development of predictive models for brain tumor diagnosis, prognosis and treatment response.

CHAPTER3

MATERIALS & METHODS

MATERIALS and METHODS

3.1 Data Set

In order to support the segmentation of complex brain tumors, the BraTS'2020 dataset employs pre-operative MRI scans obtained from multiple institutions. Access to this dataset was obtained via the CBICA Image Processing Portal, which required submission of a data request form (available at https://ipp.cbica.upenn.edu/). MICCAI 2020 BraTS data has been published by School of medicine, University of Pennsylvania. The Perleman School of Medicine's Center for Biomedical Image Computing and Analytics provided the dataset, which includes multimodal scans in the form of NifTI files (nii.gz). The scans from different patients are described as original T1-weighted (T1), Fluid-attenuated inversion recovery (T2-FLAIR), Gadolinium enhanced T1-weighted (T1Gd) and T2-weighted (T2) volumes.

Pre-processing of dataset started after acquitting it; however, there are still some necessary transformations to make in order to train it. In our case, each patient directory contains five multimodal scans such as T1, T2, Flair, T1ce, and an annotation file. In total, there are 369 cases.

To ensure consistency and accuracy of gliomas, about four annotators manually annotated each imaging dataset in the study using the basic annotation protocols. Experienced neurologists later reviewed and verified the annotations to avoid any discrepancy. Gadolinium-enhancing tumor (ET), Non-enhancing tumor or necrotizing area (NET/NCR) and the peri-tumoral edema (ED) are the annotations defined by experienced professionals.

3.1.1 Dataset Addition

Brats’20 dataset consists of 369 patient cases for training purpose. This challenging dataset had 125 cases in validation set for further evaluation. In order to check model accuracy and for better implementation of our model, we created two additional validation sets, each of them containing 33 and 40 patient cases respectively. Each validation set is created from available sets of past two years, Brats18 and Brats19 challenges that helped in comparison and better evaluation of our model performance.

3.2 Methodology

The generalized segmentation framework research is described below. SegResNet framework is used here for achieving best dice score coefficients (DSC). Three Dimensional 3T Multimodal MRI images of brain with increased soft tissue enhancement on T2CE and FLAIR and mild attenuated images on T1 and T2 are used as input images to detect the necrotic tissue and glioma occupying area by using proposed algorithm and framework. Output of the model gave segmented images and calculated the DSC of proposed model on training and validation sets along with TC, WT and ET. This section includes a pipeline for accurate image segmentation along with the details of network architecture frame. The schematic approach to image segmentation is shown in Figure.

3.2.1 Pre-Processing

Brats-20 tumors segmentation involves a sequence of steps from data gathering to inference on test images. For our DL model, the BraTS20 dataset was sourced from the Center for Biomedical Image Computing and Analytics and consists of both training and test set images. In addition, the dataset has been preprocessed to make it amenable for training and inferencing.

The good generalization ability of the model can be achieved by splitting data sets into training, validation, and a test set that significantly affects the model performance. The dataset is preprocessed when acquired; however, there are still some necessary transformations to make in order to train it. In our case, each patient directory contains five multimodal scans such as T1, T2, Flair, T1ce, and an annotation file. As discussed earlier, BraTS 2020 dataset, which contained multimodal scans in NifTI files (nii.gz) format, underwent pre-processing by converting the images to NumPy arrays. This conversion process was necessary to facilitate further analysis using Python Libraries, MONAI and PyTorch while the model used is SegResNet.

In total, there are 369 cases. Some files weren’t loadable; therefore they have been discarded, following that we got 366 cases for training. As mentioned above, each patient case has five multimodal scans that are not desirable for training. In a standard form, they should be combined such a way as to make a scan stacked with the four multimodal scans except for the annotation file.

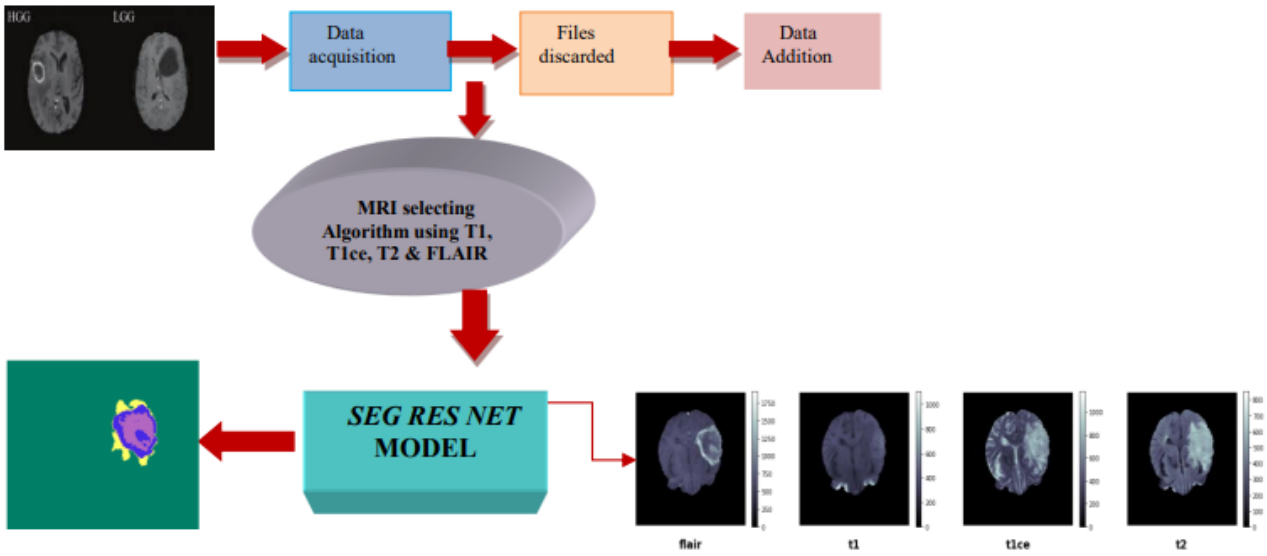

Figure 9: Schematic image of segmented model trained on input MRI images

3.2.2 Data Augmentation

The resulting scan has the shape (4, 155, 240, 240), where 4 corresponds to the four different modalities for one particular. These 4 modalities include basic MRI sequences named T1, GD-T1, T2 and FLAIR sequences. While 155 here represent the total number of brain slices in a scan, and (240, 240) is the height and width of the resulting scan.

The annotation file of each tumor has also been modified and segmented to account for the 3 different tumor cores identified as ED (peri-tumoral edema), NET/NCR (necrotizing area or non-enhancing tumor core) and ET (enhancing tumor). (Saima Rathore 2018) Instead of these labels ET, ED and NET/NCR, it's better to optimize the three overlapping regions for better understanding of segmented images. These 3 cores include enhancing tumor ET, whole tumor WT and tumor core TC respectively and are now used for better data augmentation. (Spyridon Bakas 2017, Duc-Ky Ngo 2020)

The resulting annotation file has the shape (3, 155, 240, 240) where 3 correspond to three different tumor cores ET, WT and TC. Each scan in this study consisted of a total of 155 brain slices while the height and width of the resulting scan is 240. In addition, an extra dimension will be added for each input and ground truth to account for batch size.

Some transformations have been applied to the training data to make it capture real-world and diverse cases. All the images have been normalized to 0 mean and 1 standard deviation, moreover, orientation transform has been used to normalize the orientation of images. Images have been randomly cropped for better spatial resolution using appropriate region of interest with probability *p* and intensity has been normalized for augmenting data properly. In order to reduce under-fitting or over-fitting, the input volume was randomly flipped in right-left, inferior-superior, and anterior-posterior direction with a drop-out probability of 0.5. All these images were randomly flipped across different axis for data augmentation with probability *p* while scale intensity and axis have been randomly normalized using factor *f* and probability *p*. All these transformations that have been used are listed below in Table 2.

Data Augmentation	**Value**
Orientation	True
Normalize	Normalize each scan
RandSpatialCrop	Randomly crop with an ROI size with probability p
RandFlip	Randomly Flip across different spatial axes with probability p
NormalizeIntensity	Normalize scan intensity
RandScaleIntensity	Randomly scale intensity with a probability value p and factor f

Table 2: Data Augmentation Parameters

3.2.2 Network Architecture

The model follows the encoder-decoder structure, (Myronenko 2018) which learns the deep image features in the encoder parts, followed by a decoder part that reconstructs the input image and mask. Similarly, in order to reconstruct the input image, a branch was added at the end of the decoder part that was similar to the encoder-decoder structure known. This network architecture is explained in Figure 10.

3.2.3.1 Encoder Part

The Encoder component of the model utilized a ResNet block, incorporating two convolutions, (Kaiming He 25 Jul 2016, Th´eophraste Henry 2020) Group Normalization (GN) (Yuxin Wu 2018) and Rectified Linear Unit (ReLU) (Chaity Banerjee 2019, Yuan 2020). Moreover, each block contains an additional skip connection. The green block shown in Figure 10 represents ResNet block. The input image goes through a series of stacked blocks to downsize the spatial dimensions by 2 while increasing the feature size by 2. Input is downsized by stride convolutions where all convolutions are 3x3x3 with initial filters that have been added in our model equalizing it to 16. This enhances the capability of feature learning. We have used down sample blocks 1, 2, 2, and 4 in the encoder part with input channels equal to 4.

3.2.3.2 Decoder Part

The Decoder component of the model maintained the same structure as the Encoder, but with a modification to its architecture, incorporating a single block for each spatial level. Every decoder block starts with upsizing by using 3D bilinear up-sampling feature. (F. P. Polly 2018, Myronenko 2018, Amin Zadeh Shirazi 2020) This doubles the spatial size of the original image by 2. Moreover, by using 1x1x1 convolution, numbers of features were reduced by a factor of 2. An encoder output of the same spatial size is concatenated with each block at every level of decoding. This results in the decoder output spatial shape similar to the input with an equal number of features, followed by 1x1x1 convolution in order to map it into a 3 channels output image.

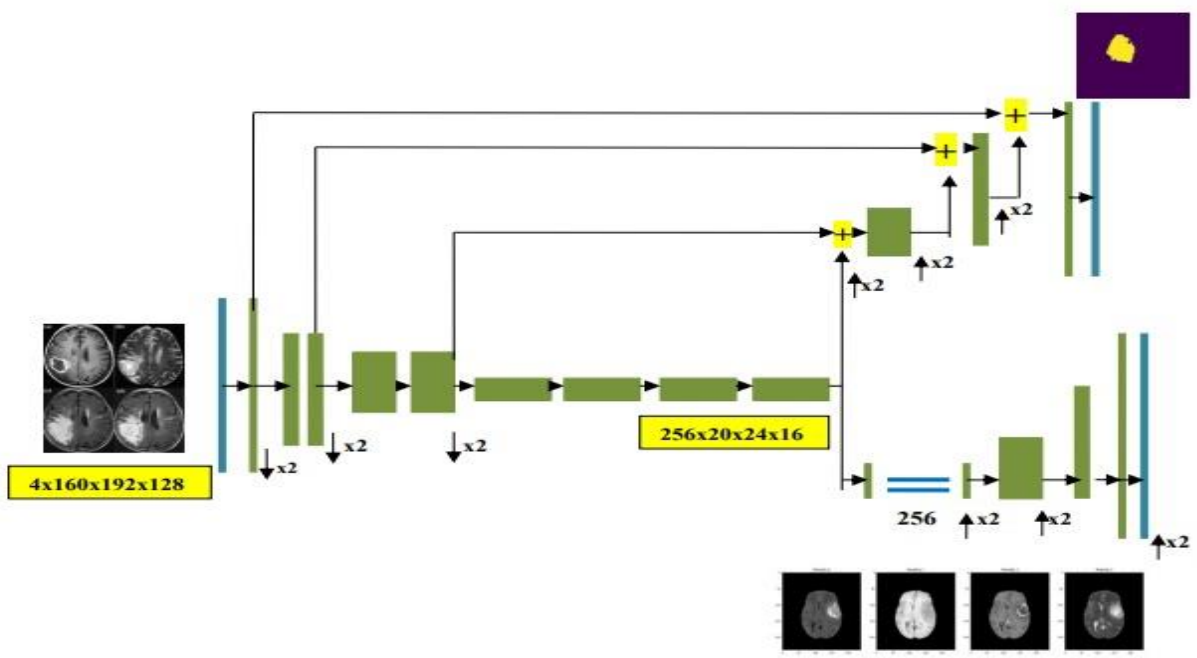

Figure 10: Output of our segmentation model. Input involves 4 channel 3D-crop with 3x3x3 convolution and stride 2. ResNet block is shown in dark green comprising of two convolutions, GN, ReLU and a skip connection. The encoder part downsizes the spatial dimensions along with increasing its features while the decoder part up-samples the spatial dimension and maps the input image to a 3 channels mask.

3.2.3 Training

After preprocessing, the next important step is to train the deep learning model on the Brats20 dataset. The data was loaded into batches for training, data generators were applied for training, validation, and test sets. We have used *SegResNet* in our model for segmentation. Since the training dataset is not enough, as a motivation a branch has been added to add regularization. The model has been trained for 100 epochs with the hyper-parameters listed in Table 3. The model has been trained on Tesla 100 GPU with a list of parameters.

Learning rate is considered to be the one of the most important hyper parameter in deep learning during training step. It is selected in such a way that model gets smallest loss value without compromising the learning speed of training dataset. For each model pre-trained weights on the SegResNet dataset that were used in our model have been trained using learning rate of $1e-4$ keeping in mind the validation loss and preventing over or under fitting of model.

The best checkpoints have been saved on each epoch with weight decay rate of $1e-5$. Images

in our trained dataset have (240,240,155) shape, however, models have been trained on SegResNet dataset with 3 channels in total while the mismatched images were skipped in first layer. Our model adds a dropout value of 0.2 that switched off 20% of neurons in second last layer in the proposed network. A data loader is created to load the dataset from google drive keeping the batch size 1 for our dataset where it is loaded for training. Since the GPU memory doesn't support batch sizes more significant than one, therefore, we used batch size of 1 to avoid Cuda out-of-memory issue. Our proposed model using SegResNet encoder-decorder architecture outperformed the other models with training set DSC of 0.90. DSC for TC, WT and ET also surpassed previous models that have been discussed in results section.

Hyper-parameters	**Value**
Learning rate	1e-4
Batch size	1
Epochs	100
Weight decay	1e-5
Image shape	(240, 240, 155)
Dropout probability	0.2
workers	2

Table 3: Training Hyper-Parameters

3.2.3 Evaluation

After training phase, the best checkpoints have been saved on each epoch and evaluation of the model can be performed by loading the best checkpoints. In this stage, LGG and HGG segmented 3T MRI images are evaluated and model ground truth and model prediction for modality is achieved. We used two separate validation sets, randomly chosen from the Brats-18 and Brats-19 respectively. Both sets contain 33 and 40 patient cases in addition to 125 patient cases of Brats-20 to evaluate the model more effectively.

3.2.5 Inference

The test set evaluation can be accomplished by using inference, which was measured by calculating the total time taken by our model. The model executed a 0.90 mean dice score on

training and 0.87 on the validation set. Thus, this shows that the model is not over-fitting or under-fitting with the given hyper-parameters on training data set. A model inference image prediction and labels are shown in Figure 11 and Figure 12.

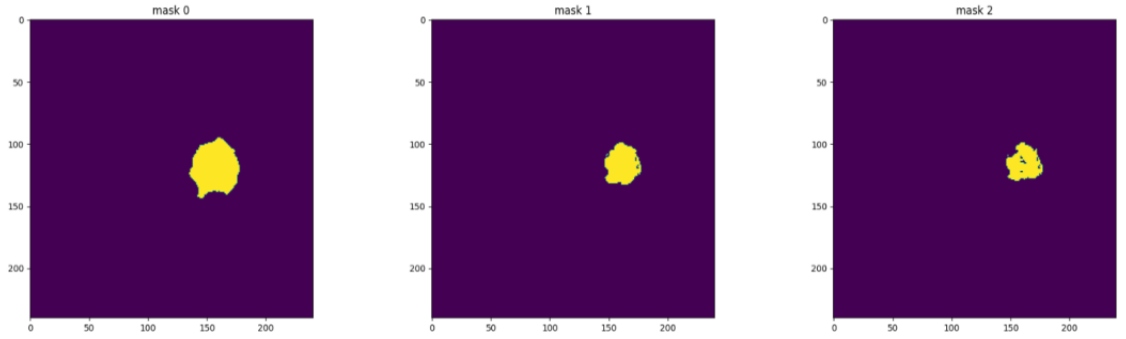

Figure 11: Model ground truth for a modality

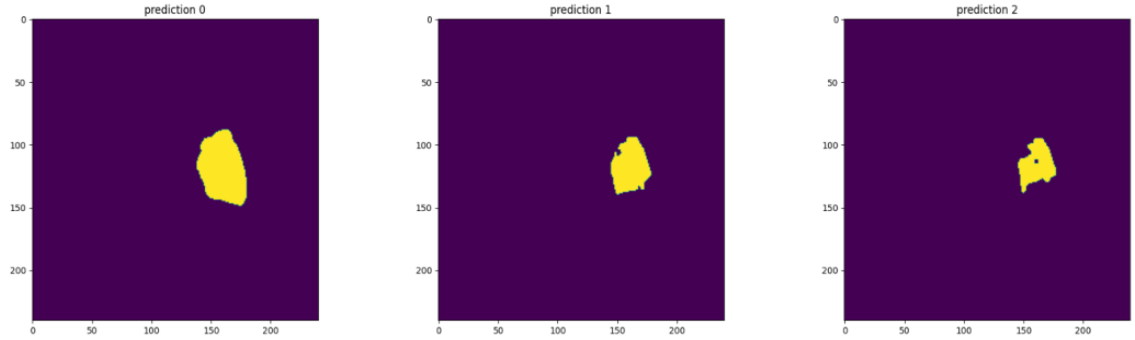

Figure 12: Model ground prediction for a modality

CHAPTER4

RESULTS

RESULTS

Our model has achieved a 0.90 mean dice score on training set and a mean dice score of 0.87 on the validation set. The performance of our proposed method on the testing set was evaluated by calculating the dice scores for tumor core, whole tumor, and enhancing tumor, resulting in an average of 0.9000, 0.8911, and 0.8426, respectively. Our results also suggest that over-fitting or under-fitting did not occur during the experiments. Our model has surpassed the previous models of BraTS'20 dataset giving highest dice scores for tumor core and enhancing tumor while second highest for whole tumor.

As already discussed in introduction section, BraTS dataset images' evaluations are done by segmentation of images using the partially overlapping whole tumor, tumor core and enhancing tumor regions instead of the three provided class label sets enhancing tumor, edema and necrosis or non-enhancing area. (Saima Rathore 2018) This can be a beneficial step in performance of proposed models reducing chances of false positive and false negative results.

Numerical values explaining impressive segmentation results and dice score coefficient of our model using SegResNet model on the BraTS 2020 test data set are shown in Table 4.

METHOD	DICE CO-EFFICIENT		
	TC	WT	ET
SegResNet	0.9000	0.8911	0.8426

Table 4: Resulting Matrices On Test Set Of Our Model

4.1 Tumor Classification

Classifying tumor before segmentation is an important and necessary step for knowing site of existing lesion. SegResNet network architecture already discussed in the methodology section learns the deep image features to classify the tumor and reconstructs the input image and mask output layer for segmentation phases.

The proposed SegResNet architecture was applied on 3T-MRI images of 2020 BraTS challenge. These multimodal images types show different tissue contrasts and intensity across different sequences, making them used widely as an unremarkable imaging technique to visualize regions of interest in the human brain, typically considering LGG and HGG. As already discussed, four MRI sequences along with an annotation file is available for each case.

Each one of these MRI modalities contains information that signifies performance improvement of our model and classifies the tumor origin. These four imaging modalities classifying the tumor location in our model are shown below explaining T2, T1, T1-contrast enhanced and FLAIR modalities.

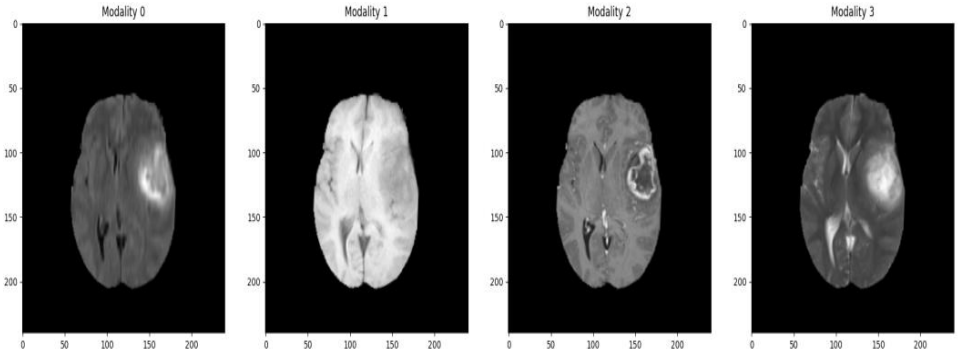

Figure 13: (a) Modality 0-T2 (b) Modality 1-T1 (c) Modality 2-T1-contrast enhanced (d) Modality3-FLAIR

4.2 Post-processing and Tumor Segmentation

Once output prediction is depicted and model prediction explains the presence of tumor, the major task is segmentation of the depicted gliomas through SegResNet model. Ground truth and image prediction for modalities are achieved after training that are explained in evaluation section. Important features are extracted from the SegResNet model detecting suitable pixels higher in intensity. These segmented image channels remove the unnecessary part of brain cells and depicts the tumor containing part in all four modalities making it easier to further segment the region of interest for glioma detection. These image channels ae further post-processed to acquire more accurate segmented images.

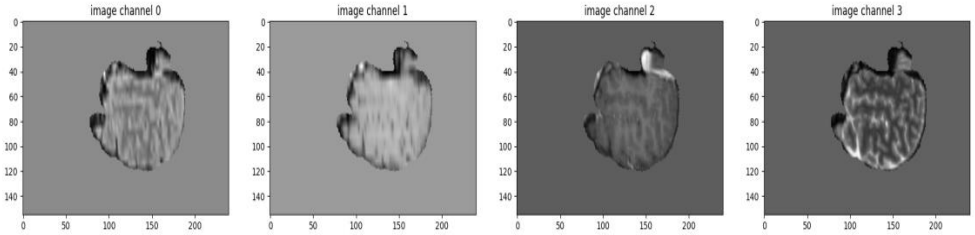

Figure 14: (a) Channel 0-T2 (b) Channel 1-T1 (c) Channel 2-T1-contrast enhanced (d) Channel 3-FLAIR

We further post-processed the segmented results by removing small unnecessary areas around the tumor corners of the 3T-MRI images making better results with some optimized pixels. Edematic area was segmented initially from T2 images provided by benchmark while FLAIR sequence was used to re-check and confirm the extended area covering edema representing "whole tumor area" and to differentiate it from other fluid-filled structures of brain.

Next major important task is to segment the complete gross tumor core that includes both enhancing and non-enhancing areas present inside whole tumor. These areas were segmented by using Gadolinium-enhanced sequence i.e, T1CE specifically for HGG- high grade gliomas. In addition toT1-ce sequences, plain T1 sequence was used for differentiation of hyper and hypo intense lesions. (Maximilian Niyazi 2016, Spyridon Bakas 2017, Saima Rathore 2018) In this way, we were able to segment contrast enhanced intensities within the gross tumor part and labelled it as "enhancing core" of the tumor. It excluded the necrotic areas from the tumor region and included only contrast enhanced region.

The hypo-intense necrotic structures within the enhancing region were visible in T1-contrast enhanced sequence. After careful subtraction of enhanced part and effected necrotizing area, the non-enhanced part of gross tumor was labeled as "tumor core". In this way, necrotic and non-enhancing part of the tumor was collectively labelled as "tumor core". (Saima Rathore 2018, Richard McKinley Oct 2019)

Graphical representation for these parameters and regions of a patient are shown in Figure 15 differentiating these regions from each other successfully after segmentation completion.

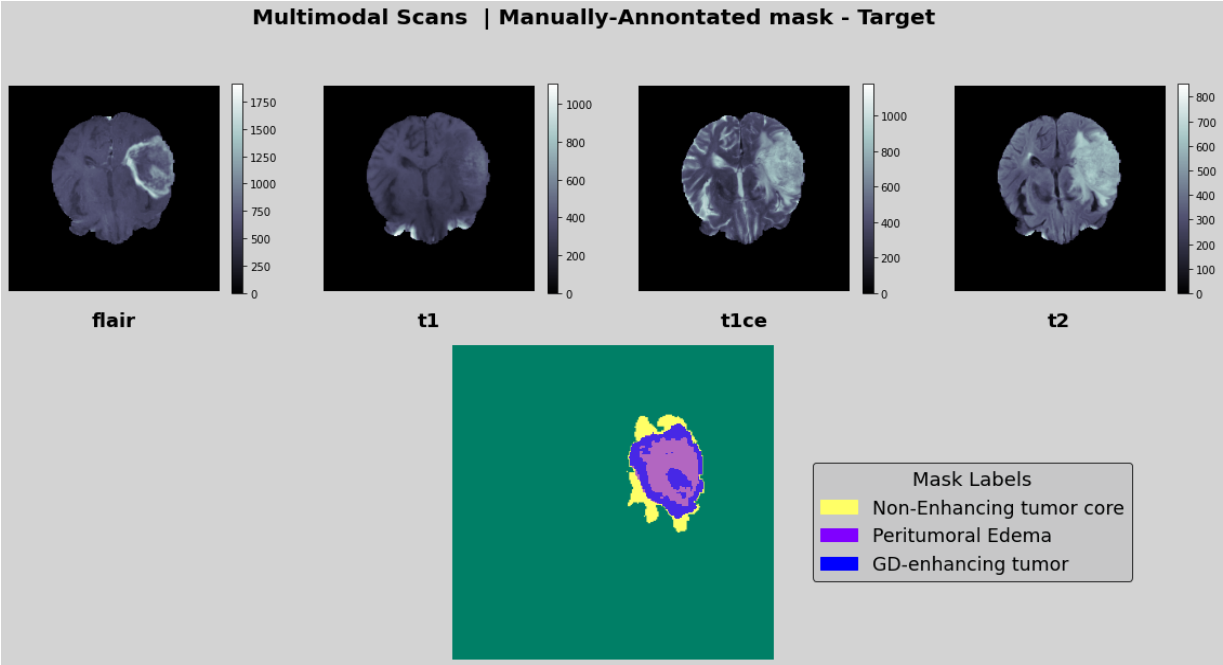

Figure 15:

(a) Yellow part explaining Tumor core TC (Non-enhancing tumor – NET/NCR)

(b) Purple region explaining whole tumor core WT (peri-tumoral edema)

(c) Blue region explains contrast enhanced region or enhancing tumor ET.

4.3 Graphical Representation

Below are the graphs showing the mean DSC on tumor core, whole tumor and enhancing tumor on our proposed model using SegResNet. In our model, Highest DSC is achieved for tumor core that depicts finest accuracy and model performance as brain gliomas are mainly depicted in tumor necrosis area.

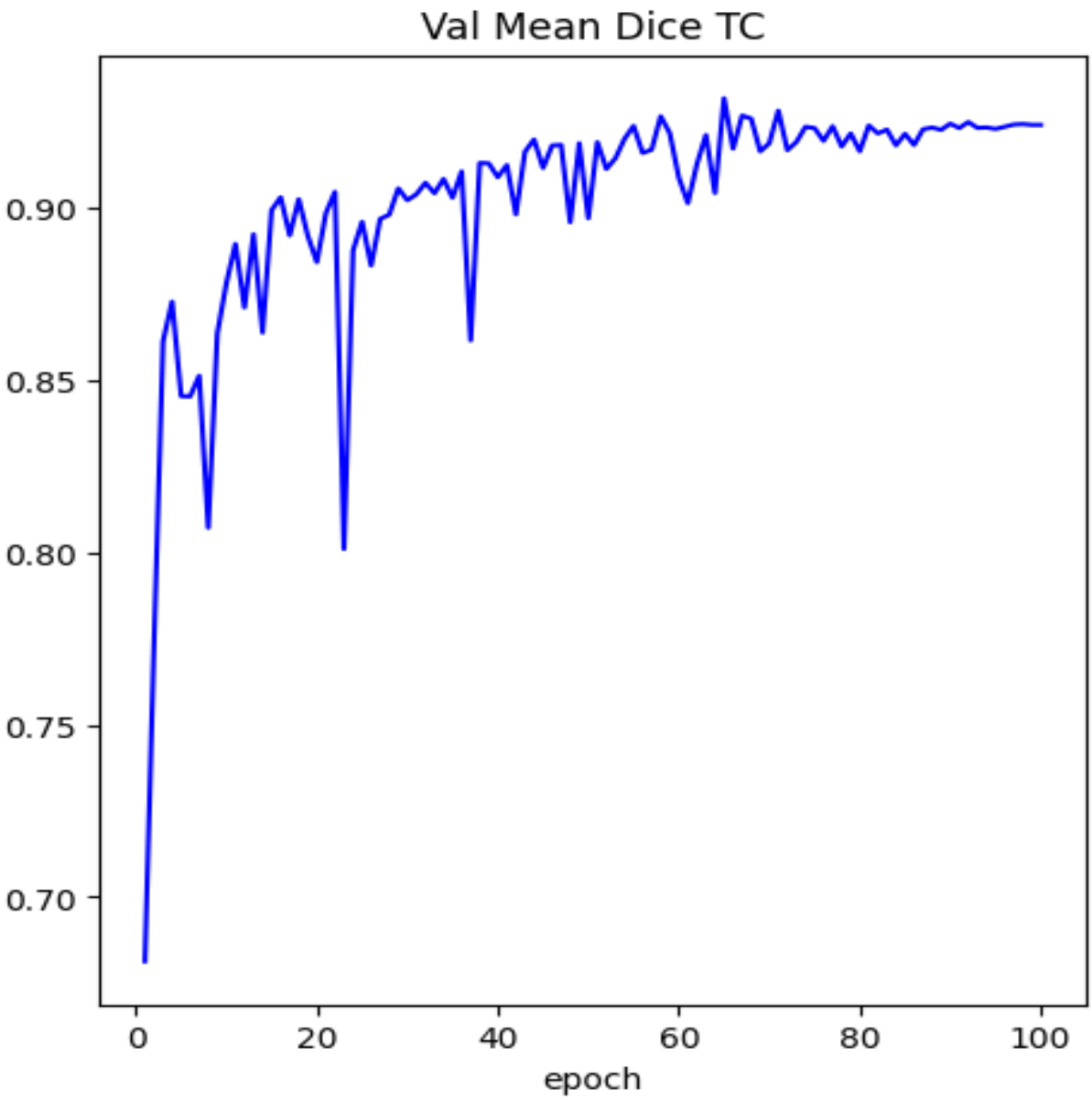

Figure 16: Graph Showing 0.90 DSC On Tumor Core TC

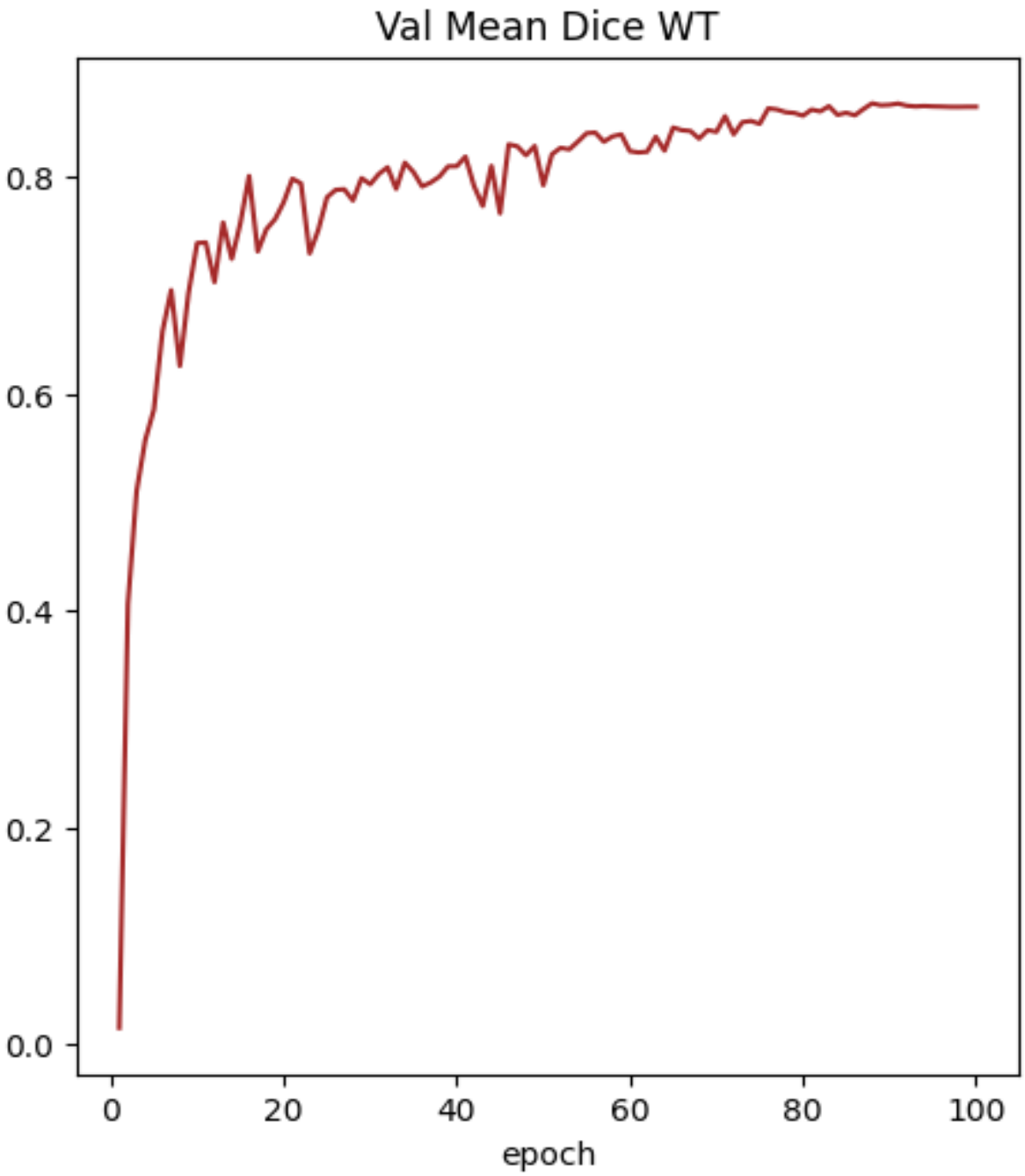

Figure 17: Graph Showing 0.8911DSC On Whole Core WT

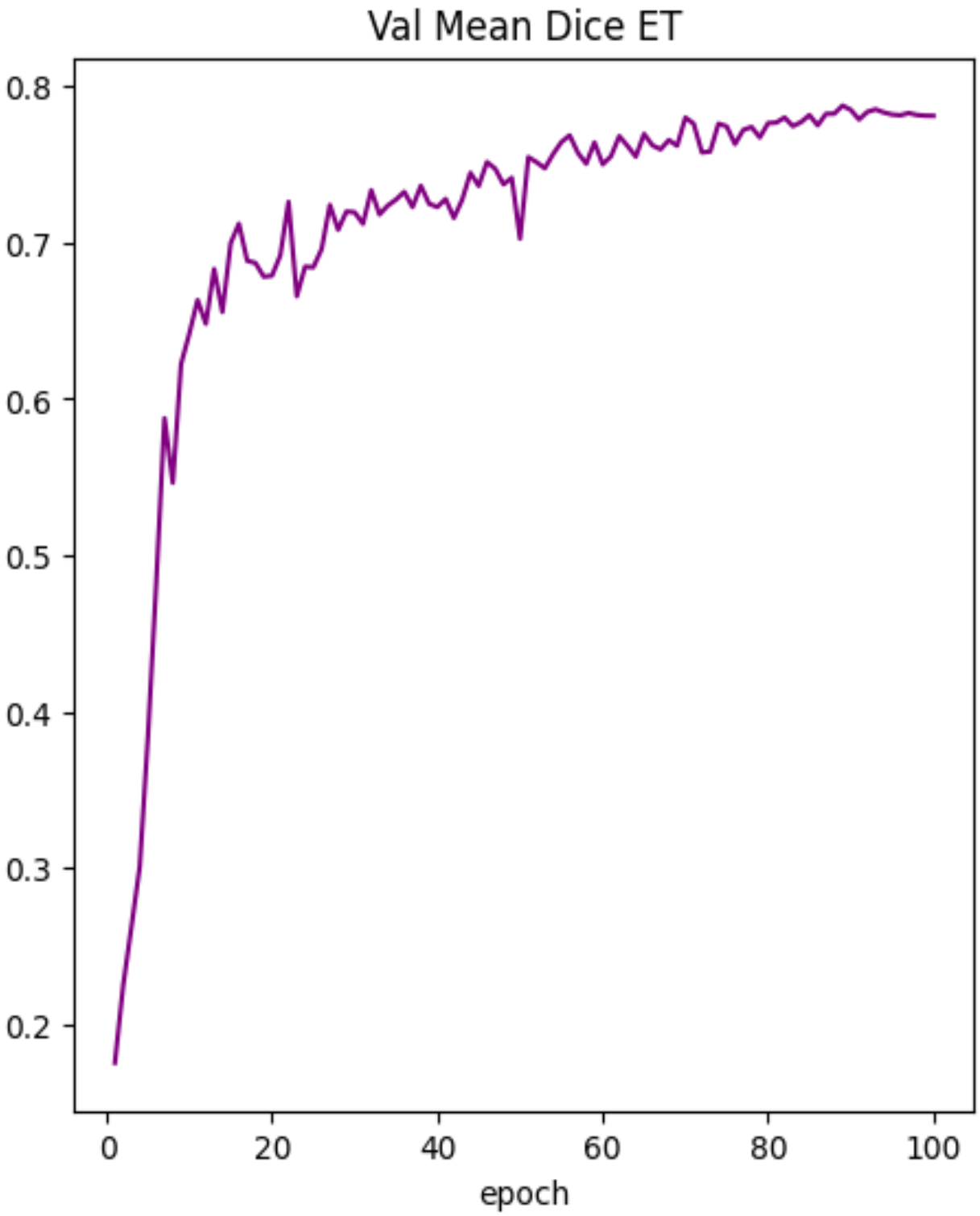

Figure 18: Graph showing DSC of 0.8426 Enhancing tumor ET

Average epoch loss depicts the error over the training set mainly in terms of mean errors for regression or segmentation images. In our model, average epoch loss was minimized due to 0.0001 learning rate and ADAM optimizer along with data loaders. Figure 19 and 20 shows the graphical representation of average loss and mean DSC on 100 epochs.

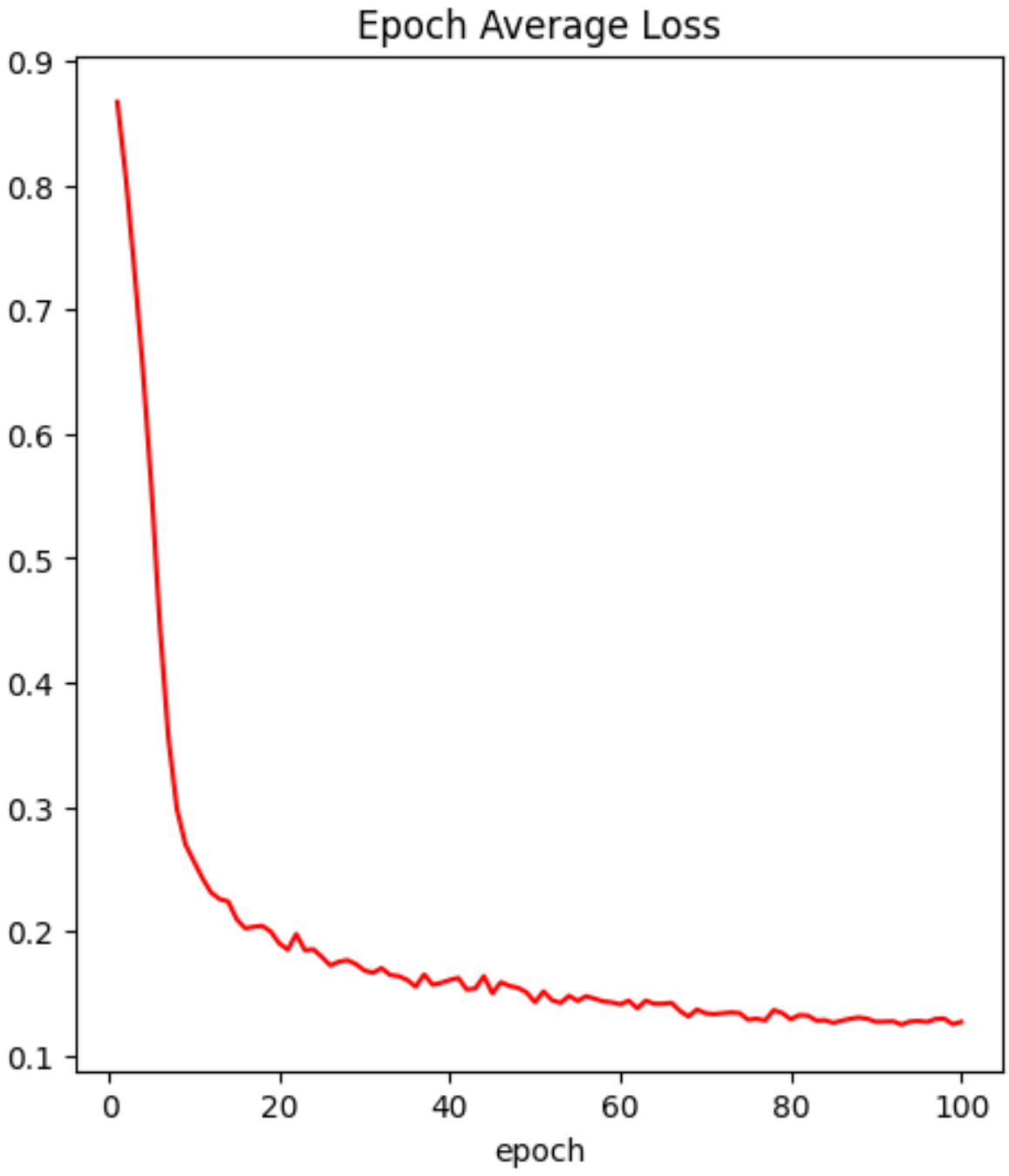

Figure 19: Average epoch loss on test-set

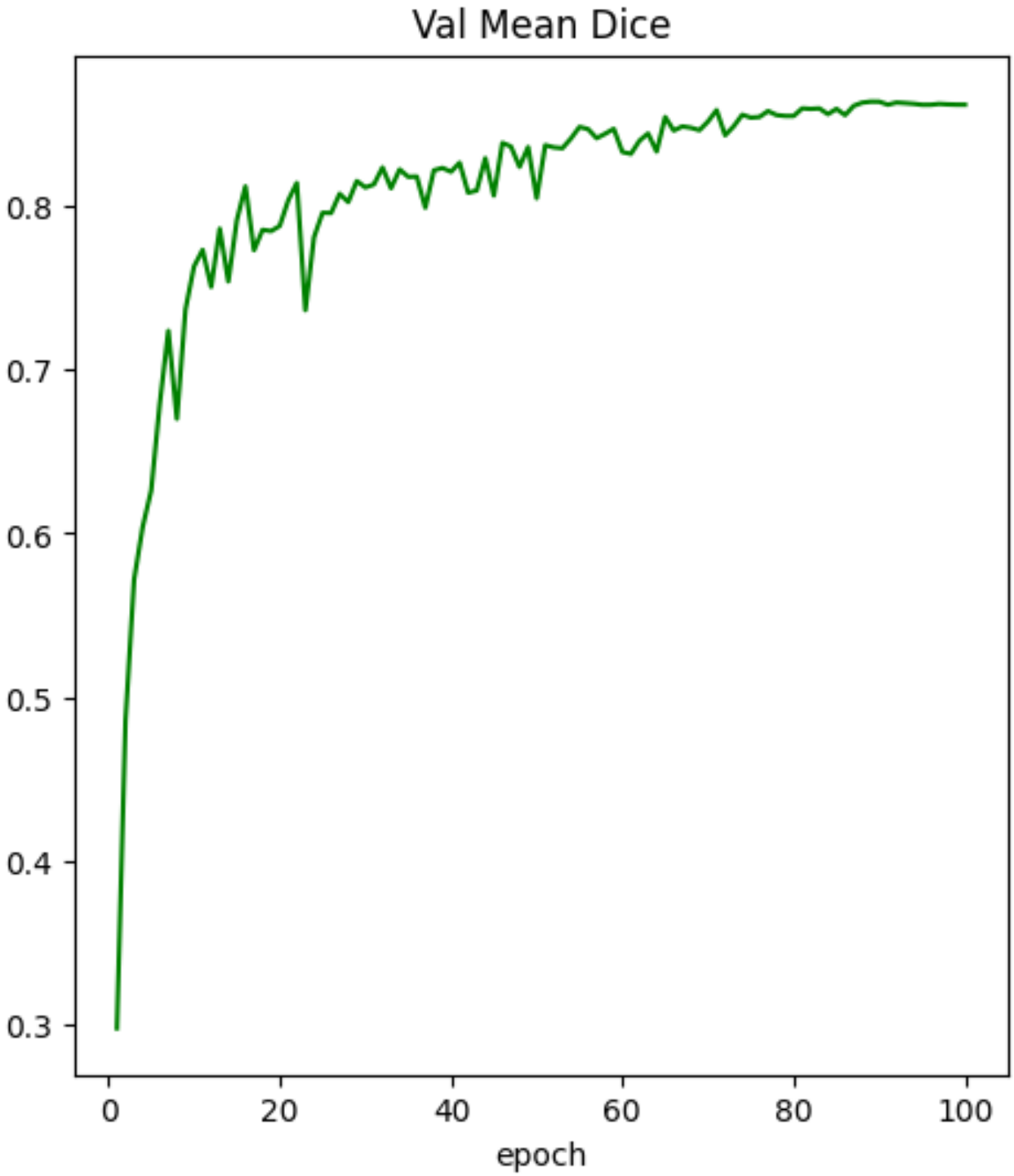

Figure 20: Mean Dice score coefficient (DSC) on Validation Set

CHAPTER5

DISCUSSION

DISCUSSION

Our manuscript describes three-dimensional segmentation of the BraTS 2020 challenge for multimodal brain tumor images containing LGG/HGG. SegResNet was used as the baseline algorithm for model development of segmented images. Using SegResNet algorithm, performance outcome received for training dataset is similar to the outline implemented for the BraTS challenge earlier. For validation set, the known BraTS method was undergone some specific modifications that created novelty comparing datasets and models of previous benchmarks. Two validation sets, containing 33 and 40 patient cases respectively from BraTS 2018 and BraTS 2019 were used in addition to the given validation set of 2020 that helped us in the evaluation of our model performance.

In addition to achieving better dice scores, this addition to validation sets from past two years' datasets, gave one more major reason that why our model has surpassed previous methods. Using SegResNet model and comparing few validation images of 2018 and 2019 datasets gives a better comparison and evaluation study, thus achieving 0.90 dice score on training set and 0.87 on validation set along with better DSC of 90.00, 89.11 and 84.26 on Tumor core, whole tumor and enhancing tumor respectively.

Fabian Isensee and Paul F. J¨ager proposed their study using nnU-Net for brain tumor segmentation and took1st position in 2020 challenge. (Fabian Isensee 2020) Their DSC were 85.06, 88.95 and 82.03 on tumor core,whole tumor and enhancing tumor respectively.
HaozheJia and WeidongCai proposed the method using H2NF-Net (Haozhe Jia 2020) while Yixin Wang and Yao Zhang explained their segmentation resutls using Modality-Pairing Learning technique (Yixin Wang 2020). These challenging teams took second place in BrasTS'20 competition with dice scores of 85.46, 91.29 and 78.75 using H2NF-Net and 84.2, 89.1 and 81.6 using Modality-Pairing Learning technique on TC, WT and ET respectively. Although H2NF-Net got highest prediction modality for WT with 91.29 DSC, but considering other hyper-parameters of training and segmentation, nnU-Net technique by Fabian Isensee got 1st position in competition.

Yading Yuan stood third in competition by proposing Scale Attention Network (Yuan 2020) achieving DSC of 84.33, 88.28 and 81.77 for TC, WT and ET respectively.

Th´eophraste Henry and Alexandre Carr´e along with their co-workers proposed deeply-supervised 3D U-net neural networks method. (Th´eophraste Henry 2020) They made their place among top 10 challengers with DSC of 84.0, 89.0 and 79.0 for TC, WT and ET respectively.

These comparisons are explained in Table 5 below.

Our results	**1st position**	**2nd position**	**2nd position (tie)**	**3rd position**	**Among Top 10**
TC: 90.00	TC : 85.06	TC: 85.46	TC: 84.2	TC: 84.33	TC: 84.0
WT: 89.11	WT 88.95	WT: 91.29	WT: 89.1	WT: 88.28	WT: 89.0
ET: 84.26	ET: 82.03	ET: 78.75	ET: 81.6	ET : 81.77	ET: 79.0

Table 5: COMPARISON WITH PAST MODELS ON BRATS 2020

CHAPTER6

CONCLUSION

CONCLUSION

Our study surpassed previous BraTS'20 competition challengers in many aspects. Our model using SegResNet was able to achieve highest dice scores for tumor core TC and ET i.e; 90.00 and 84.26 respectively while second highest dice score was achieved for WT i.e; 89.11. Multi-modal 3T brain tumor segmentation tasks are challenging in many aspects but can be accomplished with good accuracy using SegResNet architecture, with properly designing pre-processing, training and inference steps.

CHAPTER7

REFERENCES

REFERENCES

1. Al-Dhahir, F. B. M. M. A. (2022). Gliomas, StatPearls Publishing LLC.

2. Amin Zadeh Shirazi, E. F., Mark D. McDonnell, Mahdi Yaghoobi, Yesenia Cevallos, Luis Tello-Oquendo, Deysi Inca, Guillermo A. Gomez (2020). "The Application of Deep Convolutional Neural Networks to Brain Cancer Images: A Survey " Journal of personalized medicine**vol. 10,4 224**.

3. Anuja Arora, A. J., Mayank Gupta, Prakhar Mittal, Suresh Chandra Satapathy (2021). "Brain Tumor Segmentation of MRI Images Using Processed Image Driven U-Net Architecture." Computers MDPI**vol10**.

4. Bjoern H. Menze, A. J., Stefan Bauer (2014). "The Multimodal Brain Tumor Image Segmentation Benchmark (BRATS)." IEEE Transactions on Medical Imaging**Vol 34, No. 10**(0278-0062 © 2014 IEEE).

5. Chaity Banerjee, T. M., Eduardo Pasiliao Jr. (2019). An Empirical Study on Generalizations of the ReLU Activation Function. Proceedings of the 2019 ACM Southeast Conference. A. f. C. Machinery**:** 164–167.

6. Changxing Ding, Z. J., Minfeng Liu, Dacheng Tao (2019). Two-Stage Cascaded U-Net: 1st Place Solution to BraTS Challenge 2019 Segmentation Task. Brainlesion: Glioma, Multiple Sclerosis, Stroke and Traumatic Brain Injuries. BrainLes 2019. Lecture Notes in Computer Science., Springer, Cham. . **vol 11992**.

7. Crimi, A. (2015). Brain Lesions, Introduction. Brainlesion: Glioma, Multiple Sclerosis, Stroke and Traumatic Brain Injuries. BrainLes 2015. Lecture Notes in Computer Science, Springer, Cham. **vol 9556**.

8. Dinthisrang Daimary, M. B. B., Khwairakpam Amitab, Debdatta Kandar (2019). "Brain Tumor Segmentation from MRI Images using Hybrid Convolutional Neural Networks." Procedia Computer Science 167 (2020) 2419–2428.

9. Duc-Ky Ngo , M.-T. T., Soo-Hyung Kim, Hyung-Jeong Yang and Guee-Sang Lee (2020). "Multi-Task Learning for Small Brain Tumor Segmentation from MRI." Applied Sciences MDPI**Appl. Sci. 2020, 10, 7790; doi:10.3390/app10217790**.

10. F. P. Polly, S. K. S., M. A. Hossain, A. Ayman and Y. M. Jang (2018). Detection and Classification of HGG and LGG Brain Tumor Using Machine Learning. International Conference on Information Networking (ICOIN), Chiang Mai, Thailand, IEEE Xplore**:** pp. 813-817.

11. Fabian Isensee, P. F. J. a., Peter M. Full, Philipp Vollmuth, and Klaus H.Maier-Hein (2020). "nnU-Net for Brain Tumor Segmentation." arXiv:2011.00848**v1**.

12. Haozhe Jia, W. C., Heng Huang, Yong Xia (2020). "H2NF-Net for Brain Tumor Segmentation using Multimodal MR Imaging: 2nd Place Solution to BraTS Challenge 2020 Segmentation Task." arXiv:2012.15318v1 [eess.IV]**v1**.

13. Jin Liu, M. L., Jianxin Wang, Fangxiang Wu, Tianming Liu, and Yi Pan (2014). "A Survey of MRI-Based Brain Tumor Segmentation Methods." TSINGHUA SCIENCE AND TECHNOLOGY
14. ISSNll1007-0214ll04/10llpp578-595**Volume 19**.

15. Kaiming He, X. Z., Shaoqing Ren, and Jian Sun (25 Jul 2016). "Identity Mappings in Deep Residual Networks." arXiv:1603.05027 **vol3**.

16. Kelly, P. J. (2010). "Gliomas: Survival, origin and early detection." Surgical neurology international**vol1**.

17. Khushboo Munir, F. F. a. A. R. (2022). "Deep Learning Hybrid Techniques for Brain Tumor Segmentation." Sensors MDPI**Sensors. 2022; 22(21):8201**.

18. MAHNOOR ALI, S. O. G., ASIM WARIS, KASHAN ZAFAR, MOHSIN JAMIL (2020). "Brain Tumour Image Segmentation Using Deep Networks." IEEE Access**VOLUME 8**.

19. Maximilian Niyazi, M. B., Anthony J. Chalmers (2016). "ESTRO-ACROP guideline ‘‘target delineation of glioblastomas”." Radiotherapy and Oncology**VOLUME 118**(ISSUE 1): P35-42.

20. Md Zahangir Alom, T. M. T., Chris Yakopcic, Stefan Westberg, Paheding Sidike, Mst Shamima Nasrin, Brian C Van Essen, Abdul A S. Awwal, and Vijayan K. Asari (2018). "The History Began from AlexNet: A Comprehensive Survey on Deep Learning Approaches." arXiv:1803.01164**v2**.

21. Michael Goetz, C. W., Franciszek Binczyk, Joanna Polanska, Rafal Tarnawski, and U. K. Barbara Bobek-Billewicz, Jens Kleesiek, Bram Stieltjes, Klaus H. Maier-Hein (2016). "DALSA: Domain Adaptation for Supervised Learning from Sparsely Annotated MR Images." IEEE Transactions on Medical Imaging.

22. Muhammad Shafiq, Z. G. (2022). "Deep Residual Learning for Image Recognition: A Survey." Applied Sciences MDPI**12(18), 8972**.

23. Myronenko, A. (2018). "3D MRI brain tumor segmentation using autoencoder regularization." arXiv:1810.11654v3 [cs.CV]**v3**.

24. Olaf Ronneberger, P. F. T. B. (2015). U-Net: Convolutional Networks for Biomedical Image Segmentation. Medical Image Computing and Computer-Assisted Intervention – MICCAI 2015, Springer, Cham. **vol 9351:** pp 234–241.

25. Philipp Kickingereder, F. I., Irada Tursunova (2019). "Automated quantitative tumour response assessment of MRI in neuro-oncology with artificial neural networks: a multicentre, retrospective study." Lanet Oncol. 2019(May;20(5):728-740).

26. Richard McKinley, M. R., Raphael Meier, and Roland Wiest (Oct 2019). Triplanar Ensemble of 3D-to-2D CNNs with Label-Uncertainty for Brain Tumor Segmentation. Brainlesion: Glioma, Multiple Sclerosis, Stroke and Traumatic Brain Injuries, © Springer Nature Switzerland AG 2020**:** Pages 379–387.

27. Saima Rathore, H. A., Jimit Doshi, Gaurav Shukla, Martin Rozycki, Michel Bilello, Robert Lustig, Christos Davatzikos (2018). "Radiomic signature of infiltration in peritumoral edema predicts subsequent recurrence in glioblastoma: Implications for personalized radiotherapy planning." Journal of Medical Imaging 5(02):1
28. DOI:10.1117/1.JMI.5.2.021219.

29. Spyridon Bakas, H. A., Aristeidis Sotiras, Michel Bilello, Martin Rozycki, Justin S. Kirby, John B. Freymann, Keyvan Farahani & Christos Davatzikos (2017). "Advancing The Cancer Genome Atlas glioma MRI collections with expert segmentation labels and radiomic features." Scientific Data.

30. Spyridon Bakas, M. R., Andras Jakab (2019). "Identifying the Best Machine Learning Algorithms for Brain Tumor Segmentation, Progression Assessment, and Overall Survival Prediction in the BRATS Challenge." arXiv:1811.02629v3 [cs.CV]**v3**.

31. Tamimi AF, J. M. (2017 Sep 27). Epidemiology and Outcome of Glioblastoma. Glioblastoma [Internet]. D. V. S, Codon Publications.

32. Th´eophraste Henry, A. C. e., Marvin Lerousseau, Th´eoEstienne, Charlotte Robert, Nikos Paragios and Eric Deutsch (2020). "Brain tumor segmentation with self-ensembled, deeply-supervised 3D U-net neural networks: a BraTS 2020 challenge solution." arXiv:2011.01045v2 [eess.IV]**v2**.

33. Yixin Wang, Y. Z., Feng Hou, Yang Liu, Jiang Tian, Cheng Zhong, Yang Zhang, Zhiqiang He (2020). "Modality-Pairing Learning for Brain Tumor Segmentation." arXiv:2010.09277v2 [eess.IV] **v2**.

34. Yuan, Y. (2020). "Automatic Brain Tumor Segmentation with Scale Attention Network." arXiv:2011.03188v3 [eess.IV]**v3**.

35. Yue Cao, P. C. S., Christina I. Tsien, Thomas T. Chenevert, and Larry Junck (2006). "Physiologic and Metabolic Magnetic Resonance Imaging in Gliomas." JOURNAL OF CLINICAL ONCOLOGY**vol 24**.

36. Yue Zhang, P. Z., Dabin Jie, Jiewei Wu, Shanmei Zeng, Jianping Chu, Yilong Liu, Ed X. Wu and Xiaoying Tang (2021). "Brain Tumor Segmentation From Multi-Modal MR Images via Ensembling UNets." Frontiers in Radiology**volume 1 - 2021**.

37. Yuille, L.-C. C. G. P. I. K. K. M. A. L. (2018). "DeepLab: Semantic Image Segmentation with Deep Convolutional Nets, Atrous Convolution, and Fully Connected CRFs." IEEE Transactions on Pattern Analysis and Machine Intelligence **vol. 40, no. 4**: pp. 834-848.

38. Yuxin Wu, K. H. (2018). "Group Normalization." arXiv:1803.08494**v3**.